International Journal of Advance Research in Science and Engineering
Volume No. 11, Issue No. 11, November 2022
www.ijarse.com
IJARSE
ISSN 2319 - 8354

CFD ANALYSIS OF RECTANGULAR SHAPED RIBS PLACED IN DIFFERENT SHAPES ON A SOLAR AIR HEATER DUCT

Trilochan Mahato [1], Dinesh Kumar [2], Kapil Nahar [3]

[1] Research Scholar, Dept. of Mechanical Engineering

[2, 3] Assistant Professor Dept. of Mechanical Engineering

Mewar University, Chittorgarh, Rajasthan, India

dinesh23100@gmail.com

Abstract:

This research focuses on a two-dimensional numerical analysis to forecast the impact of transverse rectan-gular cross-sectioned ribs on the convective heat transfer characteristics of a solar air heater. A solar air heater is a practical tool that can be used to raise the temperature of the air by absorbing heat from the sun. It is a rectangular duct with an absorber plate on top, and heat only radiates from that surface. The thermal performance of air moving through the rectangular duct is significantly altered when ribs or baffles are added slightly below the absorber plate. The outcomes of thin (high aspect ratio) and square ribs placed in three different configurations—single wall ar- rangement, staggered arrangement, and in-line arrangement on two opposite walls—were compared. At fixed rib pitch (p) and height (e) values, Nusselt number fluctuation with Reynolds number range 6000-25000 was examined. ANSYS FLUENT R19.2, a commercially accessible piece of software, was used to do simulations of computational fluid dynamics (CFD). While running simulations under comparable circumstances, the findings were contrasted with the already-done experimental ones. In order to determine the average Nusselt number, two different approaches were used. One method extracted the local Nusselt number at numerous points and, after averaging them, produced the average Nusselt number, and the other approach was similar to the approach used in the previous experimental work. The findings showed that the addition of ribs significantly increased heat transmission when compared to a smooth duct. When the second technique of calculating the Nusselt number was used, excellent correlation was dis- covered between the findings of the previous experiments and the numerical output. However, the values obtained from the Nusselt number estimated using procedure 1 were less than those already present. The outcomes showed that the thin ribs performed better than the squared ones. Thin inline ribs, whose convective heat transfer coefficient was 1.83 times greater than that of a smooth duct, provided the highest thermal performance of the three designs.

Keywords: Solar air heater: Reynolds number: turbulent flow: Nusselt number: ribs.

I INTRODUCTION

In recent years, it has been normal practice to increase the convective heat transmission of a rectangu- lar duct with the use of baffles or ribs. This idea is frequently used to increase the thermo-hydrodynamic effectiveness

of several industrial applications, including solar air heaters, heat exchangers, air condition- ing units, freezers, chemical processing facilities, and thermal generating plants [1]. A solar air heater is a device that raises air temperature by using the heat produced by solar energy. These are affordable, basic in design, low maintenance, and environmentally friendly. The seasoning of wood, drying of agricultural goods, space heating, curing of clay/concrete construction components, and curing of industrial items are hence some of their key uses [2, 3].

A standard solar air heater has a rectangular duct form with an absorber plate at the top, a rear plate, an insulated wall under the rear plate, a glass cover over the area exposed to the sun's radiation, anda passage for air to flow through between the bottom plate and absorber [4, 5]. Figure 1.1 illustrates the intricate construction details of a solar air heater.

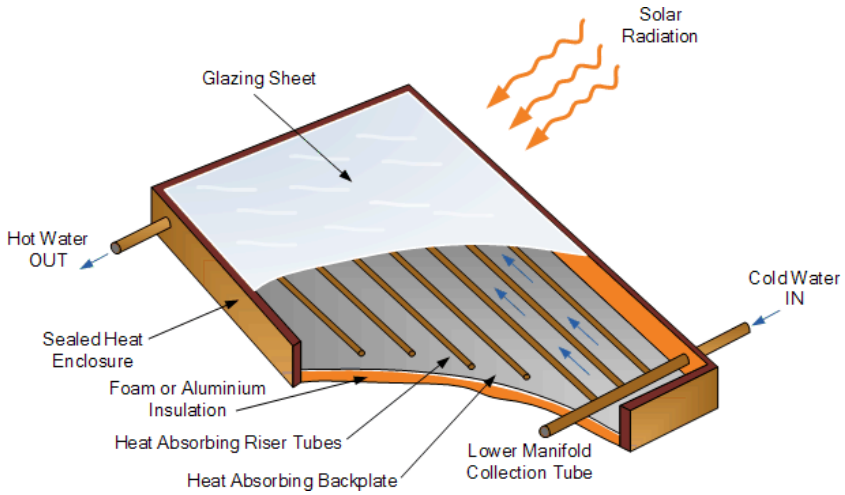

Fig. 1 Solar air heater constructional details

When the air flow via solar air heaters is between 3000 and 21000 Reynolds, the thermal effi- ciency of the device increases [3]. The duct flow is often turbulent in this region. Therefore, turbulent flow is involved in every studies relevant to the construction of an efficient solar air heater. The efficiency of conventional solar air heaters with smooth inside walls is often poor. By placing various ribs/obstacles of different forms, such as round wires, thin rectangular bars, etc. at intervals on the lower side of the collec- tion plate, the interior surface of the solar air heater may be intentionally roughened. The heat transfer rate is significantly increased as a result, but at the same time, the friction factor increases, increasing the pumping power needs.

It is well knowledge that the duct's surface roughness has a significant impact on the friction fac- tor and convective heat transfer coefficient of turbulent flow [6]. In order to achieve better convective heattransfer rates from the absorber plate to the low roughness of the air flow, artificially roughened solar air heaters must be constructed. Numerous authors are engaged in extensive research in this area, which often entails doing numerical models or tests with various types, sizes, and patterns of ribs and baffles in orderto determine the ideal set of parameters for the heater (minimum friction loss and maximum heat transfer). After doing study on solar air heaters, some scientists create a set of correlations for computing the Nus- selt number and Darcy's friction factor in terms of operational and roughness characteristics.

Breakage of the laminar sub-layer is the process through which heat transmission between the air and the

roughened absorber plate increases. By breaking up laminar sub-layers and causing local wall turbulence, ribs cause the flow to periodically reconnect and separate. Near these baffles, vortices occur, which causes the Nusselt number to substantially increase.

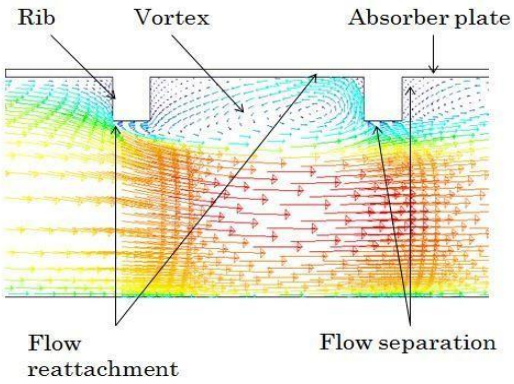

Fig. 2 Mechanism of augmentation of convective heat transfer by the introduction of ribs

II OBJECTIVE OF RESEARCH WORK

Changes in variables like air flow velocity and the interior surface roughness of the duct have a significant impact on the effectiveness of solar air heaters. These variables have a big impact on the average Nusselt number. Therefore, this idea may be positively applied to improve convective heat transfer between air flowing inside the duct and the absorber plate. Due of this, this area has already undergone extensive investigation. However, very little numerical work has been done on these projects, and the most of them have been experimental. An good way to fully comprehend how flow operates in solar air heaters with barriers present is through numerical analysis utilizing CFD soft- ware. Results using CFD are more reliable than those from experiments. Other advantages of adopting CFD software include time savings and lower expenses associated with task completion. Therefore, the goal of this research is to demonstrate that CFD can be utilized to properly design solar air heaters based on their thermal performance. This research focuses on a numerical analysis of the impact of thin transverse rectangular baffles (high aspect ratio ribs). The following chapter provides a comprehensive literature review of research on solar air heaters. Furthermore, it will be obvious from the available literature that no such research has yet been done. The review serves as the foundation for the current project's motivation, which aims to fill a gap in the literature. Therefore, a concentrated effort is needed to comprehend the thermo-hydraulic behavior of these devices in order to increase their efficiency so that systems may be precisely developed, bearing in mind the vast variety of applications of solar air heaters and turbulent flow in the area of engineering.

A. Problem Formulation

The goal of the current effort is to simulate an intentionally roughened solar air heater that circulates air in two dimensions. With the aid of transverse-square and thin (high aspect ratio) ribs, the inside surface of the air heater was roughened. On both the lower and upper faces, the ribs were organized in a variety of ways, including one wall alone, staggered, and in line.

B. Computational Modal Geometry

It was thought to be a rectangular part. It was divided into three sections: a test part measuring L2, an entry section measuring L1, and an exit section measuring L3. The two-dimensional domain was used for the numerical simulations. It comes as a result of the numerical computations Chaube et al. [23] conducted on their 7.5 aspect ratio solar air heater. On the same geometry, they compared two- dimensional and three-dimensional data, but they were unable to discern any significant differences. They provided an explanation for their finding by asserting that for continuous transverse ribs, the sec-ondary flow impact was insignificant at larger duct aspect ratios. The geometry used is comparable to the rectangular duct created by Skullong et al. [1]. Their rectangular duct measured 1500 mm in length, 256 mm in width, and 25 mm in height, with a 500 mm test section length.

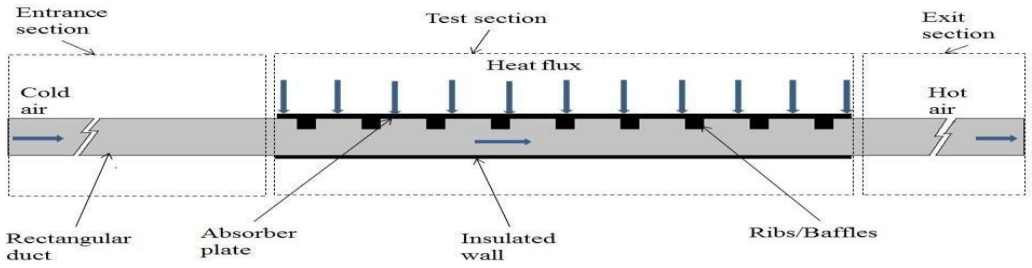

Fig. 3 shape of the computational domain

Given that an exit length more than 2.5 √WH and an entry length greater than 5 √WH were required togenerate a fully developed flow in the test domain, our domain test section's length was thus set at 500 mm. These dimensions were chosen in accordance with ASHRAE standards. The shape of the computational domain is depicted in Figure 3. In Fig. 4, the various rib configurations used for simulation are shown.

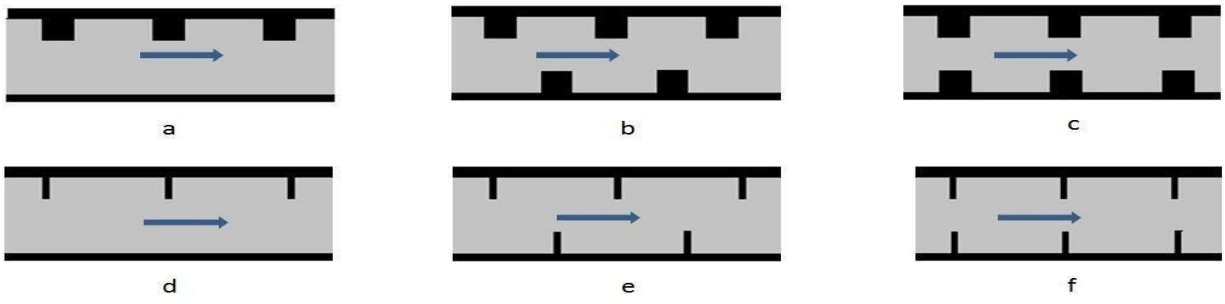

Fig. 4 Different arrangement of ribs namely (a) single square ribs, (b) staggered square ribs, (c) in-linesquare ribs, (d) single thin ribs, (e) staggered thin rib and (f) in line thin ribs

Table 1 Operating and Geometrical parameters used for CFD analysis

S.No.	Operating and Geometrical parameters	Value / Range
1.	Test length of duct, L_2	500 mm
2.	Entrance length of duct L_1	400 mm
3.	Exit length of duct L_3	200 mm
4.	Duct height, H	25 mm

5.	Duct width, W	256 mm
6.	Duct hydraulic diameter, D_h	45.5516 mm
7.	Aspect ratio of duct, W/H	10.24
8.	Constant heat flux, q"	1200 W/m^2
9.	Range of Reynolds number	6000-24000

The test duct's roughness characteristics were represented by repeated square ribs (t_t = 5 mm) and thin ribs(tb = 0.6 mm) with an axial pitch of p = 50 mm. Re was altered between 6000 and 24000 since solar air heaters perform best between these numbers. Only the upper wall of the absorber plate received a constantheat flow of around 1200 W/m2. Simulations were run on the assumption that the flow was constant. Table 1 provides a list of the geometrical and operational parameters utilized in the computational study.

C. Boundary Conditions

No-slip boundary criteria were applied to all of the rectangular duct's walls, including the one that had been roughened. The upper wall of the absorber plate's boundary condition was chosen to have a con- stant heat flow of 1200 W/m2. Boundary conditions were set up for the entrance with uniform velocity and an inlet temperature of 300 K and the exit with invariable pressure (atmospheric pressure). According to Fig. 5, all other edges were designated as walls with insulated boundary requirements.

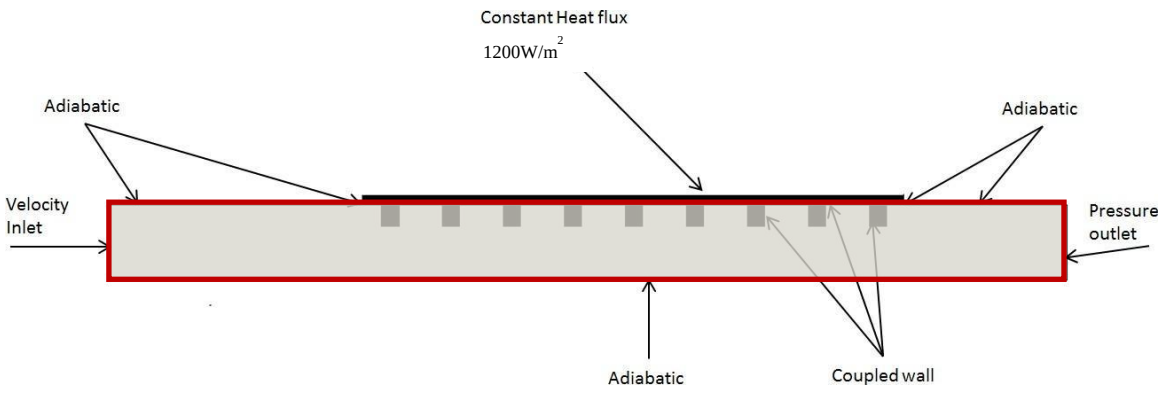

Fig. 5 various boundary requirements imposed to the computational domain's boundaries

D. CFD Modelling

Accessible through commerce The CFD Programme used to numerically solve the relevant gen- eral differential equations was ANSYS FLUENT v 19.2. This Programme uses the FINITE VOLUME METHOD to numerically simulate.

E. Geometry Formation Process

The geometry was created using the for-purchase Programme ANSYS Design Modeler R19.2. Prior to generating the surface using the "built drawings" option, an x-y plane outline of the geometry without ribs was

first made with the proper dimensions (in mm). The contact between the absorber plate and fluid was then the subject of another illustration. By selecting the second drawing as the tool geometryand using the "face-split" option, the first produced surface was divided into two faces. Following the face-splitting option, the "create surface from faces" option was used to construct surfaces from the faces. All of the surfaces and edges were then given the appropriate names.

F. Meshing of the Modal

ANSYS meshing software, which is available for purchase, was used to complete the meshing process. The resulting geometry was brought into ANSYS meshing. Each edge received the appropriate sort of "bias" and the necessary amount of divisions. The mapping facing option was turned on to produce regular rectangular-shaped mesh cells with the best orthogonal quality. After hitting the "Generate Mesh" button, the mesh was created. For various examples, the mesh domain is displayed in Fig. 6.

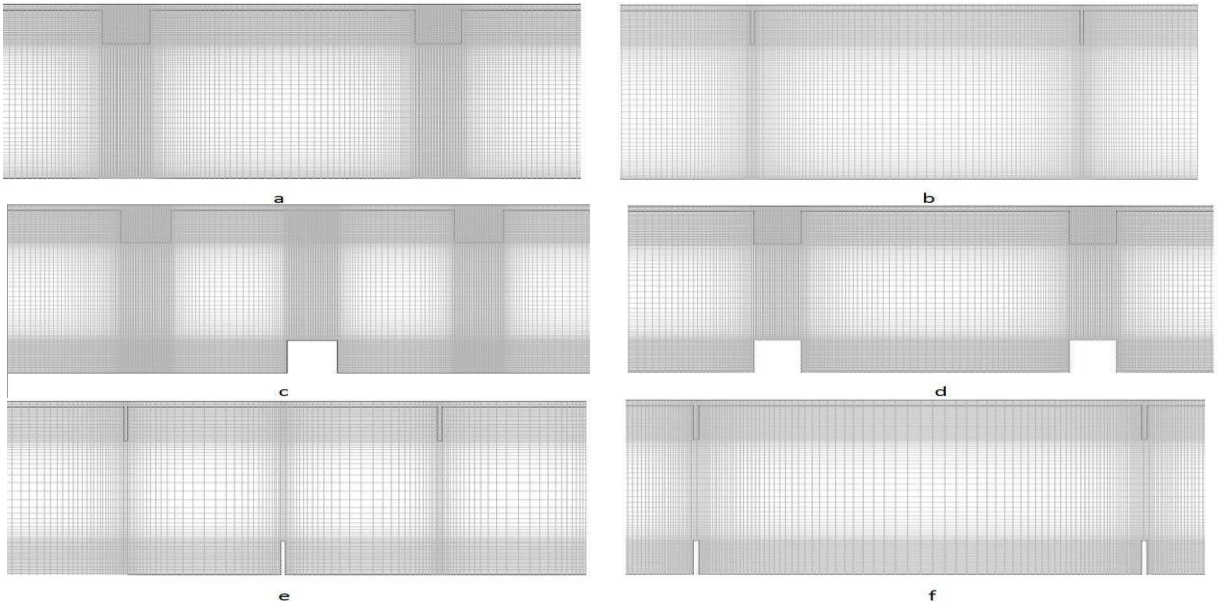

Fig. 6 2-D meshing modal of (a) single square ribs, (b) single thin ribs, (c) staggered square ribs, (d) in-line squareribs, (e) staggered thin ribs and (f) in-line thin ribs.

According to Fig. 6, the majority of the meshed domain's cells were not homogeneous in size. To prop- erly solve the relevant governing differential equations in the laminar sub-layers at these locations, fine meshing was done close to the walls. The mesh got bigger as it got closer to the center. It was made sure that the maximum aspect ratio of any grid did not exceed 10 and that the size of the grid remained consis- tent lengthwise in the entrance and exit sections of the duct.

G. Set up and flow specification

The varied flow and physical attributes were then set in FLUENT using the produced mesh. Theenergy option was turned on and the suitable turbulence model was chosen. Air served as the working fluid, while aluminum's increased absorptivity served as the absorber plate. In Table 2, their thermo- physical characteristics are listed.

Table 2 Thermophysical characteristics of air as the working fluid and aluminium as the absorber plate

S.No.	Properties	Unit	Working fluid (air)	Absorber plate (aluminum)
1.	Density	kg/m^3	1.1767	2719
2.	Viscosity	kg/m-s	1.8582e-05	-
3.	Specific heat (C_p)	J/kg-K	1006.6	871
4.	Prandtl number	-	0.714	-
5.	Thermal conduc-tivity	W/m-K	0.0262	202.4

The following presumptions were used to conduct simulations:

1. It was assumed that the absorber and duct wall were homogeneous and isotropic.
2. A two-dimensional flow that is steady, turbulent, and fully formed.
3. The thermal conductivity of the duct wall and the absorber plate was temperature independent.
4. Minimal heat losses and no heat transmission by radiation.
5. No-slip boundary conditions were assumed at the point where the wall and fluid met.
6. At a bulk temperature of 300 K, the characteristics of the absorber plate and the working fluid (air) were constant.

H. Solution

For the momentum and energy equations, the upwind scheme "second order upwind" was used. The SIMPLE method was used to relate velocity and pressure. The "Implicit Integration" solution ap- proach was used to produce temporal discretization. The relaxation parameters for pressure, density, body forces, momentum, and energy were kept at 0.3, 1, 1, 0.7, and 1 accordingly. A standard technique was used to interpolate the pressure. For all residuals, a low convergence criterion of 10-6 was set in order to properly forecast various values. Using the "Standard Initialization" option, the solution was initialised by calculating from the intake. After completing these parameters, the "Run Calculation" button was clicked to begin the iteration process.

I. Grid Sensitivity test

To get reliable findings, the proper grid size selection is crucial. In order to determine the optimal grid size to run the numerical simulations over a variety of Reynolds numbers, grid independence tests were carried out. Since the thickness of viscous laminar sub layers is lowest at Re = 20500, the grid inde- pendence test was carried out at this Reynolds number. In light of this, choosing the appropriate grid sizeat this Reynolds number would provide a grid size that successfully predicted heat transfer values throughout the whole Reynolds number range available in our simulation (Re = 6000-24000). The total number of grids used in the grid independence test was raised until there was little discernible difference between the findings of two successive grid sizes. The grid size associated with the second-to-last exampleof the grid independence test was

deemed to be the best one at this time and was utilized for subsequent simulations. Different geometries were subjected to different grid independence tests.

The outcomes of grid independence tests performed on various geometries are displayed in Figure 7. Since it was established in the preceding section that SST-k-omega most correctly represented a solar air heater, it was utilised as the turbulent model in all circumstances. When there was less than 2% fluctua-tion in the Grid Independence test results, the optimal mesh size was determined.

After this mesh size, the number of mesh cells is progressively increased. Table 3 lists the range of meshcell counts as well as the optimal number of mesh cells for each configuration.

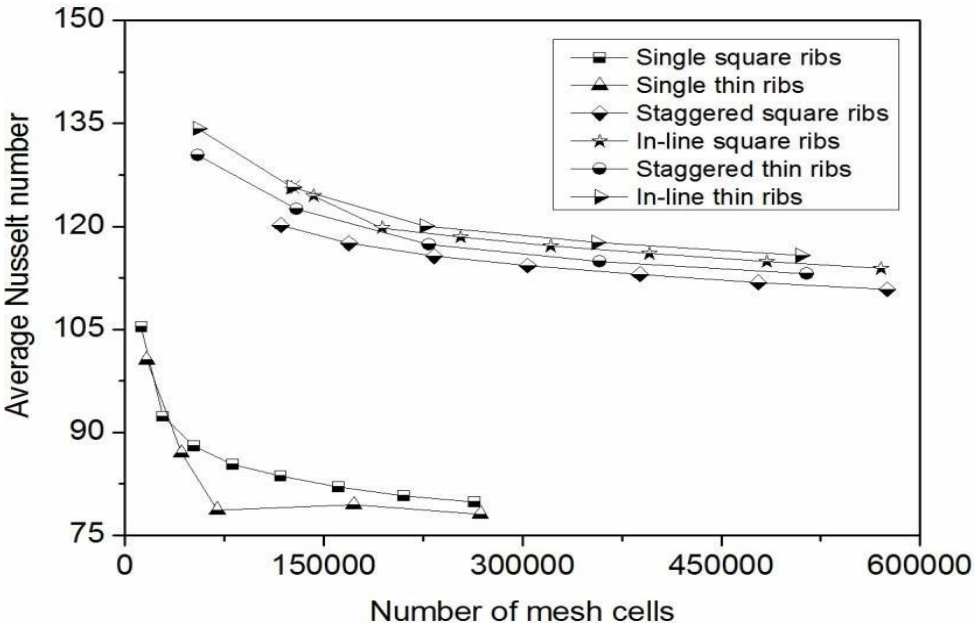

Fig. 7 The outcomes of grid independence tests performed on various geometries

Table 3 Grid Independence test results

S.No.	Rib configuration	Range of mesh cells	Optimium number of mesh cells
1.	Single square	11267 - 230179	211061
2.	Single thin	14396 - 243401	169812
3.	Staggered square	99127 - 565312	451763
4.	In-line square	130034 - 562156	469162
5.	Staggered thin	54018 - 506246	349970
6.	In-line thin	53419 - 499196	349828

III RESULTS AND DISCUSSIONS

In this research, a computer model was built to calculate the thermal performance of a solar air heater. Just below its absorber plate, it was made up of baffles or ribs. The results of the typical convective heat transfer characteristics are presented in detail in this section.

A. CFD Results for different roughened ducts at various Reynolds number:

By completing grid independence tests, the findings of which were discussed in the preceding section, the ideal grid sizes could be determined. Two techniques were used to calculate the convective Nusselt num- ber on average. Equation 3.7's first technique (method-1) averages all local Nusselt values along the lengthof the test section. The second technique (method-2) uses Eq. 3.8 and is the one that is most frequently used in experimental research to get the Nusselt number. Skullong et al. employed the second technique [1]. The results of the average Nusselt number change with Re for each of the geometries individually are clearly shown in Fig. 8. The average Nusselt number rise for all cases as Re was raised. This trend was seen because, when Re was raised, the flow became more turbulent (more inertial effects predominated over viscous effects), increasing the rate of heat transfer. When numerical results were compared to ex- perimental ones found in the literature, there was a respectable level of agreement. For square ribs, method2's computed Nusselt values and the current ones had excellent agreement, although narrow ribs showed good agreement as well.

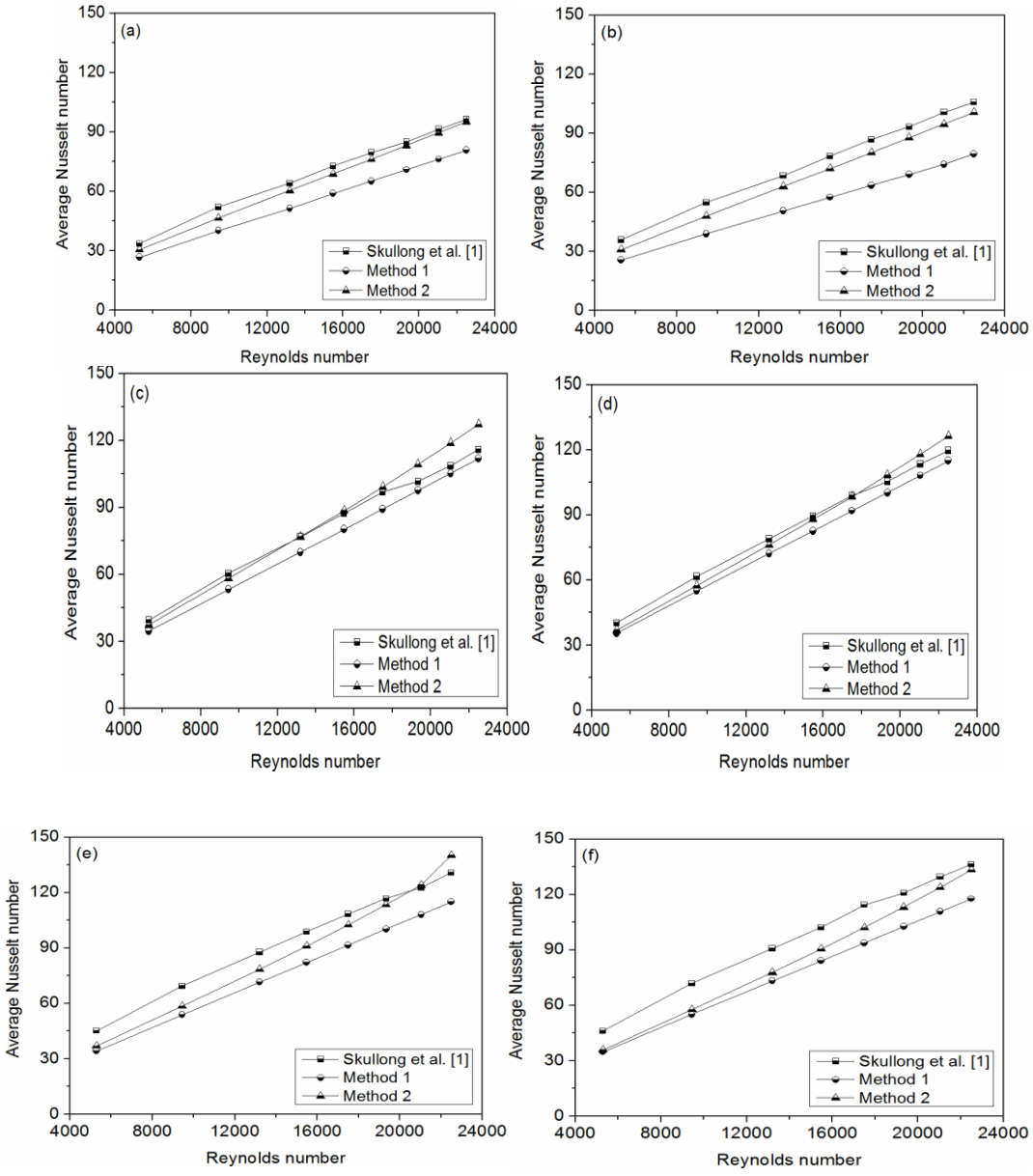

Fig 8 CFD Results for (a) single square ribs, (b) single thin ribs, (c) staggered square ribs, (d) in-line square ribs, (e) staggered thin ribs, and (f) in-line thin ribs at various Reynolds numbers

For solar air heaters with single square ribs, single thin ribs, staggered square ribs,in-line square ribs, staggered thin ribs, and in-line thin ribs, respectively, the percentage deviation of nu- merical results using method-2 from experimental results of Skullong et al. [1] was found to be approxi- mately 4.9, 8.5, 4.9, 7.7, 8.6, and 11.1 percent. For every example, it was found that the Nusselt number computed using technique 1 was far lower than the experimental ones. For solar air heaters with single square ribs, single thin ribs, staggered square ribs, in-line square ribs, staggered thin ribs, and in-line thin ribs, respectively, the corresponding percentage deviations were determined to be 18.2, 27.4, 3.15, 7.14, 16.8 and 18.6.

B. CFD Results Comparison with Various Reynolds number for all the geometries:

For all of the geometries, the comparison between Nusselt number and Reynolds number is de- picted visually in Fig. 9. The graph indicates that there was a significant increase in Nusselt number for both thin and square ribs. Strangely, skinny ribs performed far better thermally than their square counter-parts. For the entire range of Reynolds numbers employed in this simulation, in-line provided the greatest Nusselt number. The severe flow stoppage and direction change caused by in-line narrow baffles is thought to be the cause of this occurrence. In ascending order of Nusselt number, the ribbed forms are single thin ribs, including single square ribs, square ribs that are staggered, square ribs that are lined up, thin square ribs, and thin square ribs. The experimental findings showed the similar trend, with the excep-tion that the current work's single thin ribs had the lowest Nusselt values.

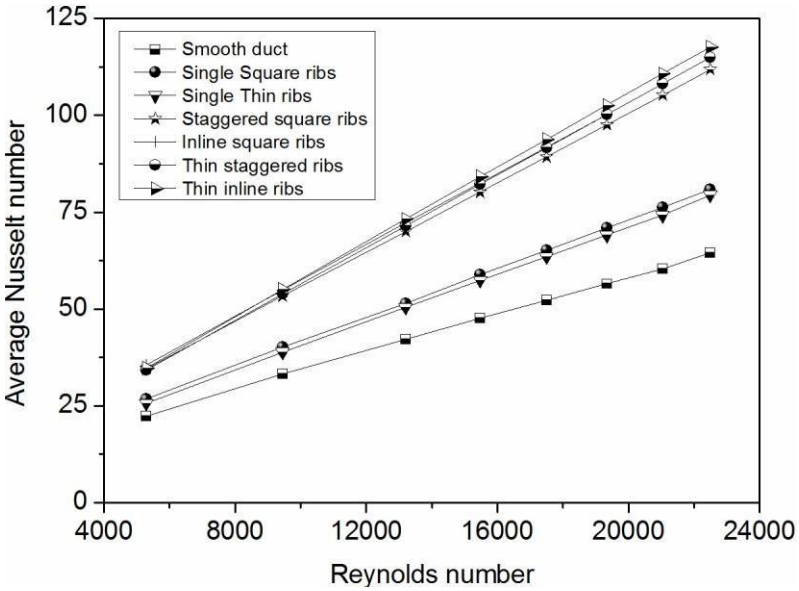

Fig. 9 Variation of Nu with Re for all the cases

C. Nusselt number enhancement (Nu/Nu_0) versus Reynolds number for separate geometries:

A solar air heater with ribs has a higher Nusselt number than one without, as indicated by the Nusselt num- ber enhancement ratio. For all of the layouts, Fig. 10 compares Nusselt number enhancement change with Re. The

optimum ratio for Nusselt number augmentation was produced by in-line narrow ribs. The highest Nu/Nu0 values for single, staggered, and in-line patterns with square ribs were 1.26, 1.74, and 1.79, respectively, whereas same values for thin ribs were 1.23, 1.79, and 1.83, respectively. This clearly shows that thin ribs have an advantage over square ones. Thin-in-line ribs were found to have the greatest value of Nu/Nu_0 at Re = 22100. Maximum Nu/Nu0 values with square ribs were 1.52, 1.81, 1.86, and 1.74 for single, staggered, and in-line designs, respectively, in the experi- mental work by Skullong et al. [1], but those with thin ribs were 1.64, 2.05, and 2.13.

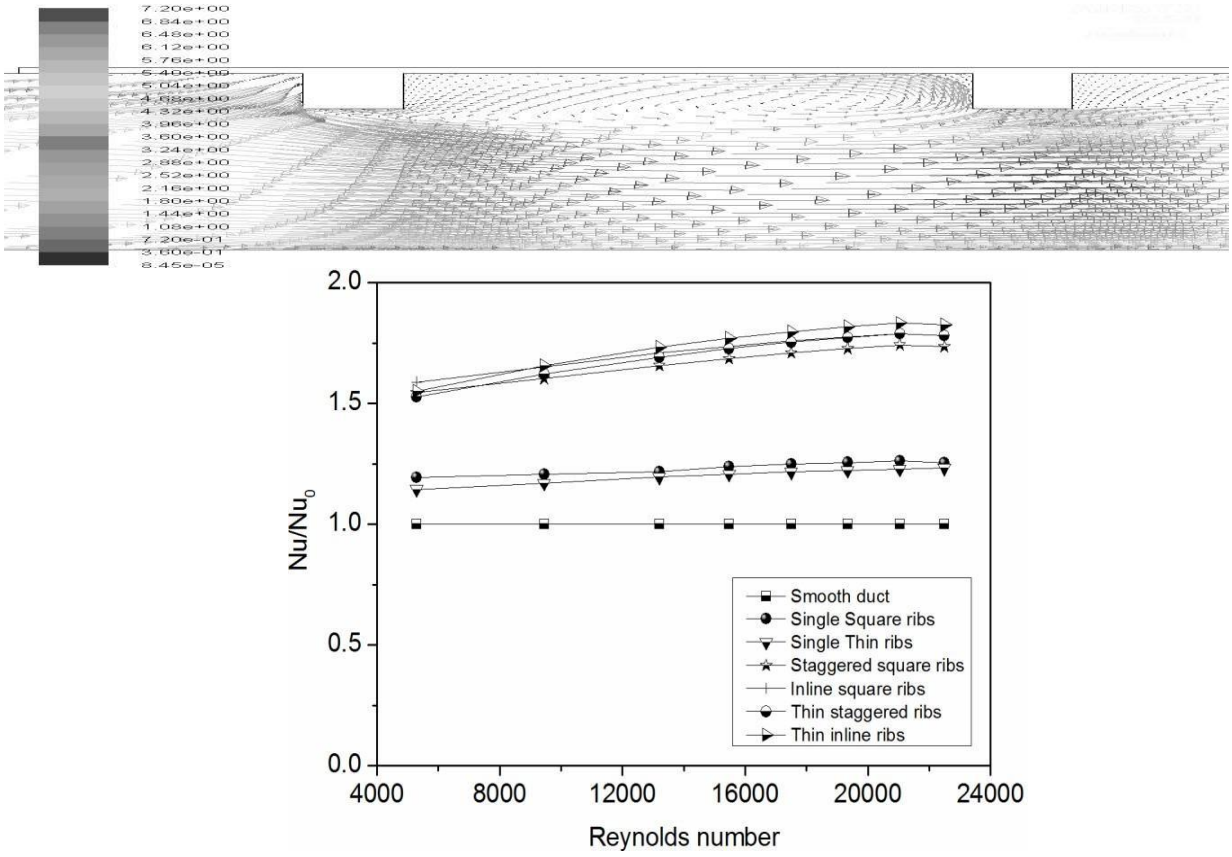

Fig. 10 Variation of Nu/Nu_0 with Re for all the cases

D. Velocity Profile

In Fig. 11, several patterns' velocity vector contour plots with a Reynolds number of 6190 are shown. The impact of ribs causes a severe irregularity in the instantaneous velocity contours. The contours map clearly depicts eddy generation close to ribs. The fluid flow suddenly expands, creating an area of separation atthe rib downstream. The fluid then reattaches itself in front of the following rib after this separation. A tiny secondary vortex develops close to the intersection of the absorber plate and fluid as a result of the flow's periodic reattachment and circulation.

In the case of narrow ribs, the secondary vortices are formed considerably more powerfully. Additionally, it is shown that as the fluid moves through the test channel, its longitudinal velocity accelerates. Thus, more disruptions are seen in the laminar sub layer, which results in a decrease in conductive heat transfer and a

notable increase in convective heat transfer.

In Fig. 4.8, the trajectories of the stream lines and the generation of vortices are shown exaggeratedly. Even if the velocity pattern in the case of staggered rib designs is more complicated, the vortices are con- siderably stronger and larger for in line setups. As a result, in-line ribs transfer heat somewhat more quickly than staggered ribs.

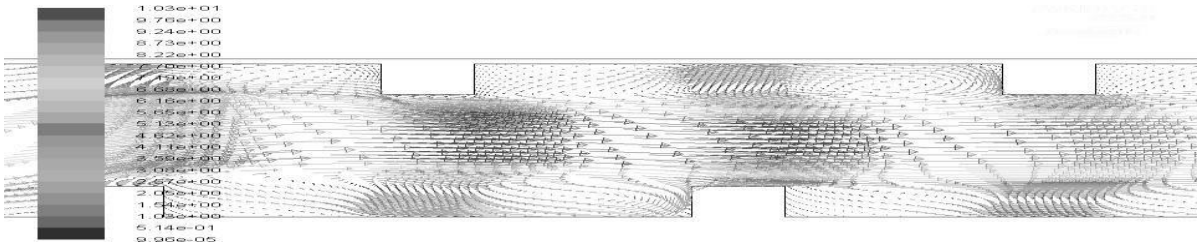

(a)

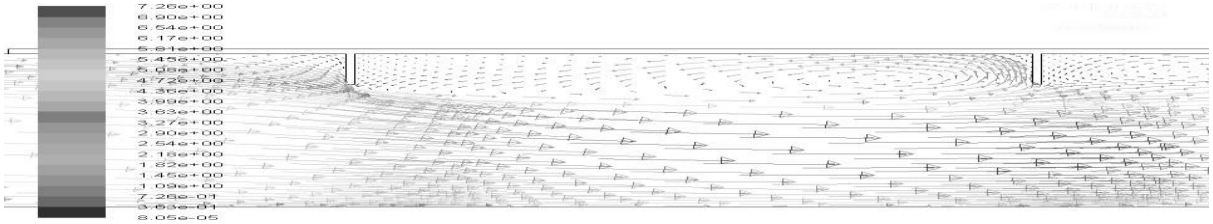

(b)

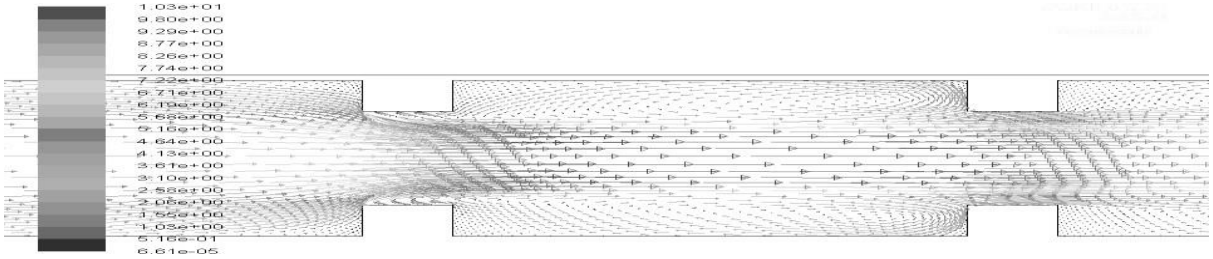

(c)

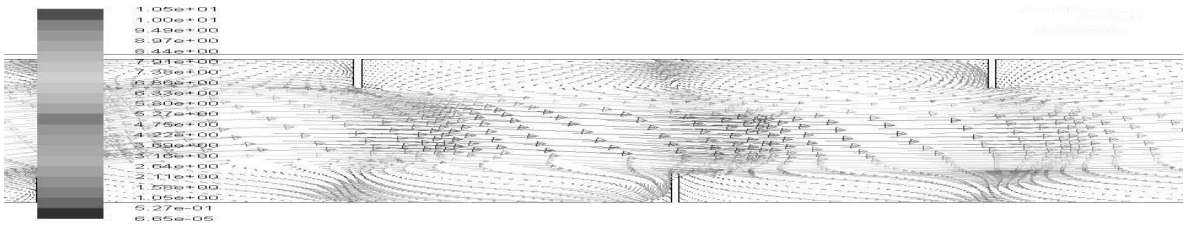

(d)

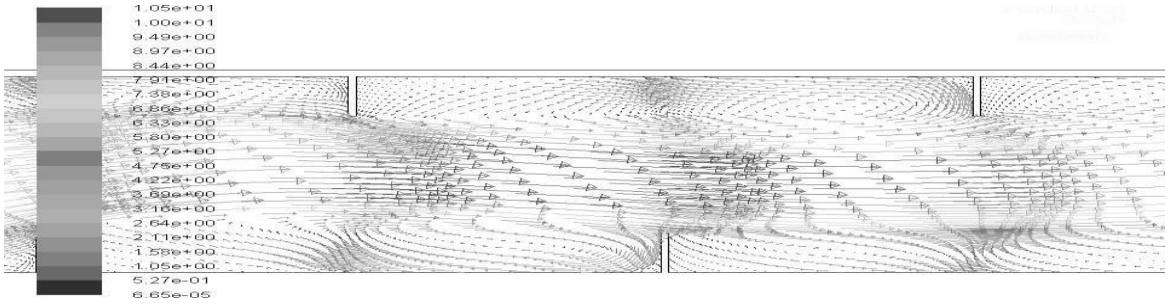

(e)

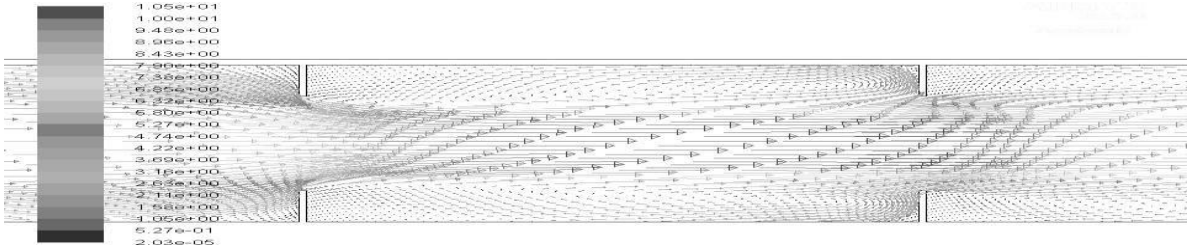

(f)

Fig. 11 Velocity vector profile of turbulent flow for (a) single square ribs, (b) sin-gle thin ribs, (c) staggered square ribs, (d) in-line square ribs, (e) staggered thin ribs and (f) in-line thin ribs.

IV. CONCLUSION

To forecast how transverse rectangular cross-sectioned ribs will affect a solar air heater's convec- tive heat transfer capabilities, a two-dimensional numerical research was conducted. Numerical analysis was done on square and thin (high aspect ratio) rib forms placed in various ways, including single wall, staggered, and in-line ribs positioned on two opposed walls, including the absorber plate, in a rectangular duct. Air served as the working medium, and only the top surface of the absorber plate received a continu-ous heat flux. These findings were drawn from the results of computer simulations.

- Increase in Reynolds number causes an increase in Nusselt number for every example that was taken into consideration for this study.
- The results showed that the thin ribs gave greater performance than the squared ones, and that there was a significant change in the heat transfer coefficient of air when ribs/baffles were placed close under the collector plate. Skullong et al. [1] also noted comparable outcomes in their own experimental studies.
- The Nusselt number was lower for the staggered ribs than it was for the in-line ones.
- The average Nusselt number was calculated using two different approaches, one of which ex- tracted the local Nusselt number at several sites and then averaged them to get the average Nus- selt number. The other method was similar to the one used in the previous experimental study. When the second technique to compute the Nusselt number was used, good agreement between the findings of previous experiments and the numerical outputs was discovered, demonstrating that CFD may be used successfully for the design of

solar air heaters. However, the initial method's calculation of the Nusselt number produced results that were less than those already in existence.

- Thin inline ribs with a convective heat transfer coefficient that was 1.83 times greater than that ofa smooth duct provided the three designs with the best thermal performance.

REFERENCES

[1] Skullong S., Thianpong C. and Promvonge, P., 2015, Effects of rib size and arrangement onforced convective heat transfer in a solar air heater channel, Heat and Mass Transfer, pp. 1- 11.

[2] Kalogirou, S. A., 2013, Solar energy engineering: processes and systems. Academic Press.

[3] Yadav A. S. and Bhagoria J. L., 2013, Heat transfer and fluid flow analysis of solar air heater: areview of CFD approach, Renewable and Sustainable Energy Reviews, 23: pp. 60- 79.

[4] Sukhatme K. and Sukhatme S. P., 1996, Solar energy: principles of thermal collection and stor-age, Tata McGraw-Hill Education.

[5] Twidell, J. and Weir, A. D., 2006, Renewable energy resources, Taylor & Francis.

[6] Cengel Y. A. and Cimbala J. M., 2006, Fluid mechanics (Vol. 1), Tata McGraw-Hill Education.

[7] Liou T. M. and Hwang J. J., 1993, Effect of ridge shapes on turbulent heat transfer and frictionin a rectangular channel, International Journal of Heat and Mass Transfer, 36(4): pp. 931-940

[8] Prasad B. N. and Saini J. S., 1991, Optimal thermo-hydraulic performance of artificially rough- ened solar air heaters, Solar Energy, 47(2): pp. 91-96.

[9] Saini R. P. and Saini J. S., 1997, Heat transfer and friction factor correlations for artificially roughened ducts with expanded metal mesh as roughness element, International Journal of Heat and Mass Transfer, 40(4): pp. 973-986.

[10] Karwa R., Solanki, S. C. and Saini, J. S., 1999, Heat transfer coefficient and friction factor corre- lations for the transitional flow regime in rib-roughened rectangular ducts, International Jour- nal of Heat and Mass Transfer, 42(9): pp. 1597-1615.

[11] Prasad K. and Mullick S. C., 1983, Heat transfer characteristics of a solar air heater used for dry-ing purposes, Applied Energy, 13(2): pp. 83-93.

[12] Prasad B. N. and Saini J. S., 1988, Effect of artificial roughness on heat transfer and friction fac- tor in a solar air heater, Solar Energy, 41(6): pp. 555-560.

[13] Verma S. K. and Prasad B. N., 2000, Investigation for the optimal thermos-hydraulic performance of artificially roughened solar air heaters, Renewable Energy, 20(1): pp. 19-36.

[14] Ahn S. W., 2001, The effects of roughness types on friction factors and heat transfer in rough- ened rectangular duct, International Communications in Heat and Mass Transfer, 28(7): pp. 933-942.

[15] Chandra P. R., Alexander C. R. and Han J. C., 2003, Heat transfer and friction behaviors in rec- tangular channels with varying number of ribbed walls. International Journal of Heat and Mass Transfer, 46(3): pp. 481-495.

[16] Murata A. and Mochizuki S., 2001, Comparison between laminar and turbulent heat transfer in a stationary square duct with transverse or angled rib turbulators, International Journal of Heat and Mass Transfer, 44(6): pp. 1127-1141.

[17] Momin A. M. E., Saini J. S. and Solanki S. C., 2002, Heat transfer and friction in solar air heater duct with V-shaped rib roughness on absorber plate, International Journal of Heat and Mass Transfer, 45(16): pp. 3383-3396.

[18] Tanda G., 2004, Heat transfer in rectangular channels with transverse and V-shaped broken ribs, International Journal of Heat and Mass Transfer, 47(2): pp. 229-243.

[19] Sahu M. M. and Bhagoria J. L., 2005, Augmentation of heat transfer coefficient by using 90 broken transverse ribs on absorber plate of solar air heater, Renewable Energy, 30(13): pp. 2057-2073.

[20] Chang S. W., Liou T. M. and Lu M. H., 2005, Heat transfer of rectangular narrow channel with two opposite scale-roughened walls, International Journal of Heat and Mass Transfer, 48(19): pp. 3921-3931.

[21] Jaurker A. R., Saini J. S. and Gandhi B. K., 2006, Heat transfer and friction characteristics of rectangular solar air heater duct using rib-grooved artificial roughness, Solar Energy, 80(8): pp. 895-907.

[22] Layek A., Saini J. S. and Solanki S. C., 2007, Second law optimization of a solar air heater having chamfered rib–groove roughness on absorber plate, Renewable Energy, 32(12): pp. 1967-1980.

[23] Saini R. P. and Verma J., 2008, Heat transfer and friction factor correlations for a duct having dimple-shape artificial roughness for solar air heaters. Energy, 33(8): pp. 1277-1287.

[24] Kumar S. and Saini R. P., 2009, CFD based performance analysis of a solar air heater duct pro- vided with artificial roughness, Renewable Energy, 34(5): pp. 1285-1291.

[25] Karmare S. V. and Tikekar A. N., 2007, Heat transfer and friction factor correlation for artifi- cially roughened duct with metal grit ribs, International Journal of Heat and Mass Transfer, 50(21): pp. 4342-4351.

[26] Sethi M. and Thakur N. S., 2012, Correlations for solar air heater duct with dimpled shape roughness elements on absorber plate, Solar Energy, 86(9): pp. 2852-2861.

[27] Promvonge P., Changcharoen W., Kwankaomeng S. and Thianpong C., 2011, Numerical heat transfer study of turbulent square-duct flow through inline V-shaped discrete ribs. International Communications in Heat and Mass Transfer, 38(10): pp. 1392-1399.